

THE DESIGN AND CONSTRUCTION OF A NOVEL DUAL-MODE DUAL-FREQUENCY LINAC DESIGN

Mamdouh Nasr*, Sami Tantawi
 SLAC National Accelerator Laboratory, CA, USA

Abstract

Accelerator structures support an infinite number of resonance modes that can be used for acceleration and yet they are mostly design-limited to single-mode operation with the fundamental mode. One promising approach in boosting accelerators efficiency is dual-mode simultaneous operation. In our work, the topic of dual-mode acceleration is studied from a wider perspective with new approaches and tools. We present a new type of accelerator structures that operates simultaneously with two modes and two frequencies. The frequencies are not constrained to be harmonically related, but rather have a common sub-harmonic.

INTRODUCTION

The idea of using multi-mode accelerating cavities have been around for a long time [1]. Also, in the past few years, there have been an effort to utilize multi-mode cavities to enhance the performance of RF electron guns as well as accelerating cavities [2–5]. All this work, however, strict the designs to harmonically related frequencies which is not optimal and even sometimes degrades the performance from that of an optimized single-frequency structures. We present a new type of accelerator structures that operates simultaneously with two modes and two frequencies. The frequencies are not constrained to be harmonically related, but rather have a common sub-harmonic. These designs will utilize a newly developed parallel-feeding network that feeds each individual accelerating cell independently using a distributed feeding network [6]. This leads to a design problem that converges to a single-cell design with identical cells. The cells are designed for maximum efficiency using new geometrical optimization that utilizes nonuniform rational B-spline (NURBS) with a series of control points. [7]

Previously, we proved that the maximum total shunt impedance for dual-mode operation equals to the summation of the individual shunt impedance for each mode under the constraint that the gradient (power) ratio equals to the individual shunt impedance ratio [8].

$$\therefore \frac{G_2}{G_1} = \sqrt{\frac{r_2 P_{L2}}{r_1 P_{L1}}} = \frac{r_2}{r_1} = \frac{P_{L2}}{P_{L1}} \quad (1)$$

where G_i , r_i , and P_{L_i} are the accelerating gradient, shunt impedance and power loss for each mode of the accelerator structure, respectively. The derivation didn't require any harmonic relation between the operating frequencies.

* mamdouh@slac.stanford.edu

SINGLE-MODE OPTIMIZATION

In our study, we investigate the optimum modes of operation for dual-mode acceleration and the enhancement of the accelerating parameters for dual-mode over single-mode operation. In this section, we start with a single-mode optimization problem to provide a reference single-mode design that we can later compare with our dual-mode designs. Also, we investigate the higher resonance modes for this single-mode design to give us an intuition on the promising higher order accelerating modes that we can consider for dual-mode operation.

We choose to set the first resonance at S-band (2.856 GHz) with an iris diameter of 5 mm, so that we can investigate second mode operation at C or X bands. We optimized for a maximum shunt impedance under the constraint of peak surface electric field-to-gradient ratio of two.

Our optimized single-mode design has a shunt impedance of 113 MΩ/m. Figure 1 shows (a) the optimized cavity shape as well as the normalized electric field distribution inside the cavity and (b) the electric and magnetic fields over the surface normalized to the average accelerating-gradient. The cavity outer dimensions and simulated accelerating-parameters are summarized in Table 1.

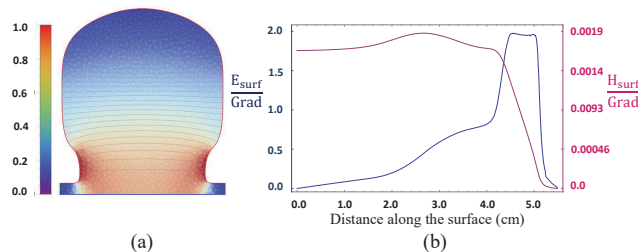


Figure 1: (a) the optimized cavity shape as well as the normalized electric field distribution inside the cavity and (b) the electric and magnetic fields over the surface normalized to the average accelerating-gradient.

At this point, we started setting up for the dual-mode optimization problem by investigating the higher-resonance-modes for the optimized single-mode design. From this we were able to identify a set of modes that can be promising for dual-mode operation. We identified the mode frequencies, total surface fields and total shunt impedance. In our calculations we use the power/gradient ratio derived in (1) for maximum shunt impedance. Figure 2 shows the mode-plots of electric field for the higher order modes each with its frequency. We studied the modes up to ~the fourth harmonic of the S-band design frequency at 2.856 GHz.

Content from this work may be used under the terms of the CC BY 3.0 licence (© 2018). Any distribution of this work must maintain attribution to the author(s), title of the work, publisher, and DOI.

Table 1: Summary of the cavity outer dimensions and accelerating parameters. The peak fields are calculated for average gradient of 100 MV/m.

Frequency	2.586 GHz
a	0.25 cm
b	4.13 cm
p	3.67 cm
R_{shunt}	113 M Ω /m
Peak E_{surf}	200 MV/m
Peak H_{surf}	0.2 MA/m
S_c [9]	4.25 W/ μm^2
Surface Loss	3.26 MW

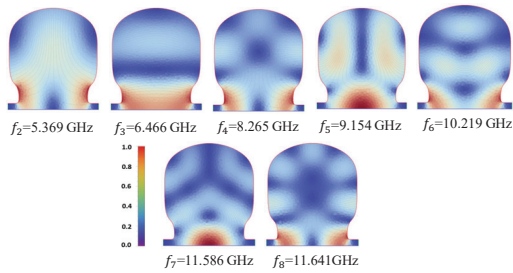


Figure 2: The mode-plots of the electric field mode-plots for the higher order modes of the optimized S-band design and their frequencies. It should be noted that the modes have either even or odd symmetry around the geometrical symmetry line.

Table 2 provides some important accelerating parameters for each one of the displayed modes when operating simultaneously with the fundamental mode. From the table we can have some conclusions and insights. First, we can notice that the increase in the shunt impedance for dual-mode operation is up to 23% over single-mode operation, keeping in mind that we only optimized for a single-mode and thus it is expected that we can obtain even more enhanced result if we optimized for dual-mode operation. Also, we can see that even with such increase in the shunt impedance, there is only small change in the peak surface fields as they are dominated by the fundamental mode.

From the table we identified four modes of particular interest for further investigation. Modes 2 and 8 are interesting because their resonance frequencies are close to a second and fourth harmonic from the fundamental one, respectively, as well as their reasonable shunt impedance value. These frequencies are close to the frequency standards of 5.712 and 11.424 GHz which give them an advantage from the source availability point of view. On the other hand, modes 3 and 4 are interesting because of their high shunt impedance.

We need to mention that we are not constraining ourselves to harmonic frequencies, but instead we aim an optimum design with a reasonable sub-harmonic. Generally, what really matters is the common sub-harmonic frequency as it defines the minimum bunch spacing for multi-bunch operation. If we assume that we have a stepped 400 ns pulse with a flat

Table 2: Parameters summary for the first eight resonance modes including the fundamental one. The total values are calculated for dual-operation with the fundamental mode.

n	f_n (GHz)	$\frac{f_n}{f_1}$	Max $\left[\frac{E_{s,tot}}{G} \right]$	R_s	$R_{s,total}$
1	2.856	1	2.00	113	-
2	5.369	1.88	2.16	13	126
3	6.466	2.26	2.29	26	139
4	8.265	2.89	2.17	25	138
5	9.154	3.21	1.99	3	116
6	10.219	3.58	2.13	1	114
7	11.586	4.06	2.02	3	116
8	11.641	4.08	2.20	12	125

gradient of 200 ns and we need to have a train of ten bunches in this period. Then, the bunch spacing need to be around 20 ns which requires a minimum common sub-harmonic frequency of 50 MHz. This can be easily achieved by tweaking our final design for maximum common sub-harmonic.

DUAL-MODE OPTIMIZATION

In the previous section, we managed to identify four modes of interest for dual-mode operation. In this section, we optimize for dual-mode operation. In other words, our target is to maximize the total shunt impedance under a constraint on the total peak field over the cavity surface. We ran four optimizations for the dual-operation of the fundamental mode with one of the four specified modes. We fixed the fundamental frequency to S-band (2.856 GHz) and the iris diameter to 5 mm. All the designs were constrained to peak electric field-to-gradient ratio of two over the cavity surface. The optimized shapes and mode-plots for each optimization case are presented in Fig. 3. As expected, the optimization resulted in different final shapes that shows correlation with the field distribution of the second-mode. Table 3 also shows a brief geometrical and accelerating parameters comparison between the designs.

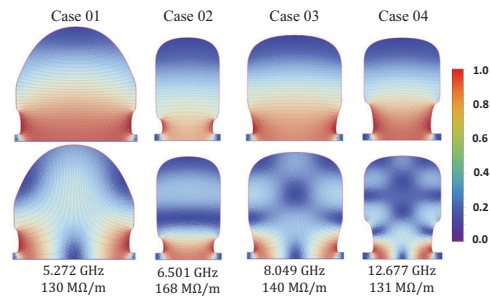


Figure 3: The final design shapes and mode-plots for each dual-mode optimization case.

From these results we can have the following observations:

1. For case 01 and 04 the resonance frequencies for the second modes of the final designs are not closer to 5.712 and 11.424 GHz, respectively. Also, the designs show

Table 3: A Brief Comparison Between Dual-mode Optimized Cases

	Case 01	Case 02	Case 03	Case 04
2nd Freq (GHz)	5.272	6.501	8.049	12.677
p (cm)	4.05	2.59	3.76	2.98
R_{s2}/R_{s1}	0.266	0.626	0.325	0.267
Total R_{shunt} (M Ω /m)	130	168	140	131

a small enhancement in the shunt impedance compared to the previous results from Table 2.

- Case 02 have the highest achieved total shunt impedance with a significant increase of 50% over the optimized single-mode design.

Given these results, we can conclude that case 02 provides the optimum dual-mode design among the studied cases. This design utilizes a TM₀₁₀-like and TM₀₂₀-like modes with a phase shift between cells of around $\pi/2$ and 1.138π for the first and second modes, respectively. Figure 4 shows the plots of snapshots of the total surface fields at different time instants during the common sub-harmonic period. We should point out that, for dual-mode operation, the peak fields repeats over the large period of the common sub-harmonic leading to a lower root-mean-square value of the surface fields.

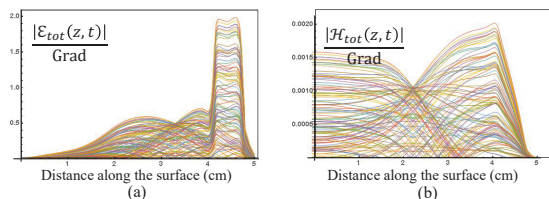


Figure 4: The absolute total (c) electric and (d) magnetic surface fields at different time instants during the common sub-harmonic period.

Table 4 presents the parameters for the selected dual-mode design showing the percentage difference compared to the parameters of the optimized single-mode design from Table 1. We can see that for the same peak fields, the dual-mode design enhances the shunt impedance by 49% and at the same time reduces the S_c -factor (used in breakdown characterization) by 35% and the wall losses by 53%. As a result, the dual-mode operation will increase the efficiency of operation due to the significant increase in the shunt impedance. It should also have much lower breakdown rates because of the reduction in the average Poynting vector over the cavity surface as well as the wall losses.

As we mentioned before it is important to have a high common sub-harmonic of the final design, however this can be easily achievable by simple tweaking of the final design. So, as a final optimization stage we did a slight change in the outer curvature of the accelerator cell and the outer radius is adjusted accordingly to keep the first resonance at 2.586

Table 4: Summary of the cavity outer dimensions and accelerating parameters for the selected dual-mode design utilizing TM₀₁₀ and TM₀₂₀-like modes. The peak fields are calculated for average gradient of 100 MV/m.

Frequency	2.586+6.501 GHz	
f_{common}	3 MHz	
a	0.25 cm	
b	4.06 cm	
p	2.59 cm	
R_{shunt}	168 M Ω /m	+49%
Peak E_{surf}	200 MV/m	
Peak H_{surf}	0.2 MA/m	
S_c [9]	2.77 W/ μm^2	-35%
Surface Loss	1.54 MW	-53%

GHz. This changed the second resonance to 6.3467 GHz achieving by this a common sub-harmonic of 317.33 MHz with almost exact parameters as in Table 4. This will allow for a minimum bunch spacing of ~ 3 ns for a multi-bunch operation.

CONCLUSION AND FUTURE WORK

The dual-mode operation of accelerator structure provides much enhanced performance that achieves much enhanced shunt impedance and lower input power requirement. This can be achieved by not-limiting the operation of these structures to harmonically related frequencies, but rather ones that share a common sub-harmonic that is suitable for multi-beam operation. The next steps in our development is to produce a full design for the dual-mode accelerator by developing the parallel-feeding network that feeds each individual accelerating cell independently for each of the dual-accelerator modes.

REFERENCES

- [1] C. E. Hess, H. A. Schwettman, and T. I. Smith, "Harmonically resonant cavities for high brightness beams", *IEEE Transactions on Nuclear Science*, vol. 32, no. 5, pp. 2924–2926, Oct. 1985.
- [2] J. Lewellen and J. Noonan, "Field-emission cathode gating for rf electron guns", *Physical Review Special Topics-Accelerators and Beams*, vol. 8, no. 3, p. 033502, 2005.
- [3] S. V. Kuzikov, A. A. Vikharev, J. L. Hirshfield, Y. Jiang, and V. Vogel, "A Multi-Mode RF Photocathode Gun", in *Proc. 2nd International Particle Accelerator Conference (IPAC'11)*, San Sebastian, Spain, Sep. 2011, paper TUPC060, pp. 1135–1137.
- [4] Y. Jiang and J. Hirshfield, "Multi-harmonic accelerating cavities for rf breakdown studies", in *Proc. 4th International Particle Accelerator Conference (IPAC'13)*, Shanghai, China, Sep. 2013.
- [5] S. V. Kuzikov, S. Y. Kazakov, Y. Jiang, and J. L. Hirshfield, "Asymmetric bimodal accelerator cavity for raising rf breakdown thresholds", *Phys. Rev. Lett.*, vol. 104, p. 214801, May 2010.

- [6] S. G. Tantawi, Z. Li, and P. Borchard, “Distributed coupling and multi-frequency microwave accelerators”, Jul. 5 2016, US Patent 9,386,682.
- [7] M. Nasr and S. Tantawi, “New geometrical-optimization approach using splines for enhanced accelerators performance”, presented at 9th Int. Particle Accelerator Conf.(IPAC’18), Vancouver, Canada. Apr.-May 2018, paper THPMK049, this conference
- [8] Mamdouh Nasr, Sami Tantawi, “A novel dual-mode dual-frequency linac design”, in *Proc. 8th Int. Particle Accelerator Conf.(IPAC’17)*, Copenhagen, Denmark, 14-19 May, 2017, paper TUPAB132, pp. 1634–1636.
- [9] A. Grudiev, S. Calatroni, and W. Wuensch, “New local field quantity describing the high gradient limit of accelerating structures”, *Physical Review Special Topics-Accelerators and Beams*, vol. 12, no. 10, p. 102001, 2009.